Model for artificial ionospheric duct formation due to HF heating

G. M. Milikh,[1] A. G. Demekhov,[2] K. Papadopoulos,[1] A. Vartanyan,[1] J. D. Huba,[3] and G. Joyce[4]

Received 28 January 2010; revised 22 February 2010; accepted 26 February 2010; published 2 April 2010.

[1] Strong electron heating by the injection of highly powerful HF waves can lead to the formation of ionospheric plasma density perturbations that stretch along the magnetic field lines. Those density perturbations can serve as ducts for guiding natural and artificial ELF/VLF waves. This paper presents a theoretical model of duct formation due to HF heating of the ionosphere. The model is based on the modified SAMI2 code, and is validated by comparison with two well documented experiments. One experiment, conducted at the SURA heating facility, used the low orbit satellite DEMETER as a diagnostic tool to measure the electron and ion temperature and density along the overflying satellite orbit close to the magnetic zenith of the HF-heater. The second experiment, conducted at the EISCAT HF facility and diagnosed by the EISCAT Incoherent Scatter Radar, measured the vertical profiles of the electron and ion temperature between 150–600 km. The model agrees well with the observations, and provides a new understanding of the processes during ionospheric modification. **Citation:** Milikh, G. M., A. G. Demekhov, K. Papadopoulos, A. Vartanyan, J. D. Huba, and G. Joyce (2010), Model for artificial ionospheric duct formation due to HF heating, *Geophys. Res. Lett.*, *37*, L07803, doi:10.1029/2010GL042684.

1. Introduction

[2] It is well known that the presence of field aligned density structures plays a critical role in the propagation of whistler waves in the ionosphere. The density structures serve as ducts for VLF/ELF waves since the density gradient perpendicular to the magnetic field can lead to their total internal reflection [*Streltsov et al.*, 2006]. Such density structures have often been observed [*Carpenter et al.*, 2002] to extend over distances covering entire magnetic field lines. They are known to trap and guide whistler-mode waves between conjugate regions [e.g., *Koons*, 1989].

[3] The possibility for creating such trans-hemispheric ducts artificially was discussed by *Perrine et al*. [2006], where a 1D model which simulates the plasma along an entire magnetic dipole field line was used. It was shown that long term continuous HF heating of the F-region by powerful ionospheric heaters, such as HAARP, generates a strong thermal wave in the ionospheric and magnetospheric plasma. The thermal wave propagates along the magnetic field line through the topside ionosphere and magnetosphere, driving ion outflows, displacing the ambient plasma and leading to the formation of density ducts that stretch along the magnetic field line to the conjugate point. We have recently generalized the previous 1D computational model to a 2D model by incorporating simulations of the plasma in the latitudinal direction. The new model allows one to describe the ionospheric parameters in both vertical and latitudinal directions with much better resolution than the old one. Therefore the new model allows for close and useful comparisons with data obtained by radars and satellites that the old model does not allow. The key objective of this paper is to validate this new model based on SAMI2. To accomplish this we will check the model against two recent well diagnosed experiments which detected large scale ducts caused by the HF heating. One experiment was conducted at the SURA heating facility and used the low orbit satellite DEMETER [*Berthelier et al.*, 2006a, 2006b] as a diagnostic tool [*Milikh et al.*, 2008; *Frolov et al.*, 2008] to measure the electron and ion temperature and density along the satellite orbit close to the magnetic zenith of the HF-heater. Another heating experiment, conducted at the EISCAT HF facility and diagnosed by the EISCAT Incoherent Scatter Radar (ISR) [*Rietveld et al.,* 2003], measured the vertical profiles of the electron and ion temperature between 150–600 km.

[4] The letter is organized as following: the next section describes the numerical model applied. In the discussion section the model output is compared with the EISCAT radar and DEMETER observations followed by conclusions.

2. Numerical Model of Formation of the Artificial Ducts

[5] The theoretical/computational model is based on the SAMI2 code developed at the Naval Research Laboratory [*Huba et al.*, 2000]. The code is a Eulerian grid-based code, which describes an ionosphere made up of seven ion species. The equations of continuity and momentum are solved for the electrons and each ion species, with the temperature equation solved for the electrons and H^+, He^+, and O^+ species. The electron density is determined on the basis of charge neutrality. The code includes $E \times B$ drift of the field lines with frozen-in plasma (in altitude and longitude), an empirical neutral atmosphere model, horizontal winds, photo-deposition into the ionosphere, ion chemistry models, and ion inertia. This inclusion of ion inertia is critical since it allows for the study of sound wave propagation in the plasma. The SAMI2 model is inter-hemispheric and can simulate the plasma along the entire dipole magnetic field line (for the geometry of the model see *Perrine et al.* [2006]). The most recent version of the SAM12 code (release 0.98) which allows description of processes at high latitudes was used here. HF heating of the ionosphere is a complex phenomenon.

[1]Department of Physics and Department of Astronomy, University of Maryland, College Park, Maryland, USA.
[2]Institute of Applied Physics, Russian Academy of Sciences, Nizhny Novgorod, Russia.
[3]Naval Research Laboratory, Washington, DC, USA.
[4]Icarus Research, Inc., Bethesda, Maryland, USA.

0094-8276/10/2010GL042684

It begins with the HF absorption which pumps the ionospheric turbulence that in turn generates the plasma heating [*Gurevich et al.*, 1996; *Gustavsson et al.*, 2001]. Since the SAMI2 code does not consider wave propagation and absorption we introduced in the model a flexible source of electron heating, as we did it in an earlier paper by *Perrine et al.* [2006]. This source of the electron heating was presented in the form of localized heating rate per electron

$$q = \frac{\mu P}{V n_e} f(x,z) = 260 \mu P(MW) \left(\frac{10km}{a}\right) \left(\frac{300km}{z_{up}}\right)^2 \cdot \frac{1}{\tan^2 \Theta} f(x,z) K/s \quad (1)$$

Here P is the power of the HF heater, V is the volume of the HF absorbed region, n_e is the electron density in this region, while μ is the absorption efficiency. f(x, z) describes the spatial distribution of the HF beam power density taken as

$$f(x,z) = e^{-\left(z-z_{up}\right)^2/a^2} e^{-\ln 2\left[(x-x_0)^2/b^2\right]} \quad (2)$$

The center of the heated region is taken at the upper hybrid altitude z_{up}. Furthermore, b is the half-power beam width near the upper hybrid point. The HF-irradiated spot is taken as a circle centered at x_o having the angular half-widths Θ so that $b = z_{up} \tan \theta$, and the HF-irradiated volume is $V = \pi a b^2$. Finally, it is assumed that electron heating occurs in an altitude range having the vertical extent a between the wave reflection point and the upper hybrid height, which is dominated by the anomalous absorption [*Gurevich et al.*, 1996].

[6] In this paper we will model the ionospheric conditions at Tromso during 10/07/99 at the time of the EISCAT experiment [*Rietveld et al.*, 2003]. We therefore use in the SAMI2 code the corresponding A_p and $F_{10.7}$ indexes, and assume that the heating began 10/7/99 at 19:24 UT. The radiated HF power was 960 kW, the half power beam width was 12°, and the facility was operated at a frequency of 4.5 MHz. Furthermore, for the unperturbed profile of the electron density we find that the reflection height for the 4.5 MHz frequency is located at 280 km, while the upper hybrid height is at about 10 km below. Thus the vertical extend of the anomalous absorption region is taken as a = 10 km.

[7] Before proceeding we should caution the reader on the timescale of model validity. The model neglects the horizontal transport caused by the **E** × **B** drift, which has a time scale $t_{dr} = b/v_{dr}$, where v_{dr} is the drift velocity and b is the horizontal scale of the heated region. Taking into account that the Tromso HF-heater has a half-power beam width of 12° and that the electron heating occurs at an altitude of 280 km, we obtain that the horizontal scale of the heated region is b = 60 km. Moreover during the time of the discussed experiments the detected drift velocity was 200–300 m/s [*Rietveld et al.*, 2003]. Thus the **E** × **B** drift led to energy loss followed by the reduction of the heating effect on a time scale of 3.5–5.0 minutes.

2.1. Simulation Procedure

[8] The code starts up from empirically determined initial conditions 24 hours before the specific heating time, and runs for 24 hours of 'world clock time'. This practice allows the system to relax to ambient conditions, and reduces noise in the system due to the initialization. Furthermore, the neutral density model was adjusted so that the computed f_0F_2 peak matched the observed. Then the "artificial heater" turns on and begins to pump energy into the electrons, using the specified parameters for that run. Artificial heating continues for some time continuously pumping energy into the electrons at the specified altitude, and the perturbations in ion and electron properties are tracked as they travel along the field line. Then the heater switches off, allowing the ionosphere to relax back to ambient conditions. The latter may also vary according to the natural factors which determine the ionosphere dynamics. This procedure minimizes noise due to the initialization and allows for the perturbations in the ionosphere to travel along the field lines, and the ionosphere to relax following strong heating. It describes the plasma response to the removal of the artificial heating as well as to its application.

[9] In order to isolate and measure the perturbations directly, a duplicate set of runs was made, identical to the run described, but with a different heating rate defined by factor q in equation (1). In addition, one run without artificial heating was performed. We refer to this as "ambient" or "reference" run, while those with artificial heating are "heated" runs. The ionosphere changes during a simulation due to natural causes, so the perturbations in the heated runs due to artificial heating would not be easily identifiable on their own. But since the same natural variations are present in the ambient data, scaling (or subtracting) by the ambient data provides a simple way to decouple the natural variations from the heater induced perturbations.

3. Discussion

3.1. Comparison With Tromso Experiments

[10] In order to reproduce results of the ISR observations made at Tromso we conducted some runs using the specified conditions at Tromso 10/7/99. Namely, we considered the index A_p = 5, and that the HF heating began at 19:24 UT. For the specified heater and antenna characteristics at EISCAT equation (1) gives that q = 12,400 μ, K/s. In our runs the heating rate varied in the range 2,000–8,000 K/s which corresponds to the absorption efficiency μ = 0.16–0.64. Note that *Gustavsson et al.* [2001] used the radar data collected during the heating experiments at Tromso to estimate the heating rate per electron as 3,000 K/s. This value corresponds to the absorption efficiency μ = 0.25, which is within the range of our estimates.

[11] Figure 1 shows the height profile of the electron density normalized to its ambient value computed at different times for a given pumping rate q = 8,000 K/s which corresponds to an absorption efficiency μ = 0.64. The heating was switched on at 19:24:00 UT for 8 minutes. The traces labeled 1 to 3 correspond to times separated by 3 minutes starting at 19:25:46, i.e. 1 min and 46 s into the heating. The trace 4 corresponds to cooling over 2 minutes and 49 seconds. Figure 1 reveals that the electron heating increases the plasma pressure and thus pushes the plasma from the heated region along the magnetic field line. Consequently, the plasma density in the heated region drops by more than 20%, but on a timescale larger than 5 minutes, as shown by the trace 3.

[12] Figure 2 shows the results of our model superimposed onto the observation results presented by *Rietveld*

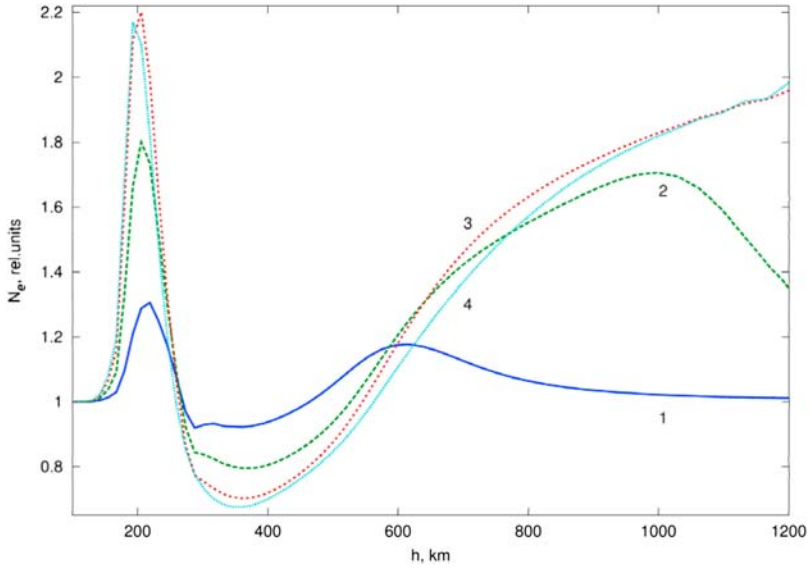

Figure 1. The electron density normalized to its ambient value computed at different times for a pumping rate q = 8,000 K/s which corresponds to the absorption efficiency $\mu = 0.64$. The heating was switched on at 19:24:00 UT for 8 minutes. The traces labeled 1 to 3 correspond to times separated by 3 minutes starting at 19:25:46, i.e. 1 min and 46 s into the heating. The trace 4 corresponds to cooling over 2 minutes and 49 seconds.

et al. [2003, Figure 3]. The latter were made by the EISCAT ISR at 19:28 UT. Figure 2 (left) shows the observed altitude profile of the electron density (circles) and that computed by the SAMI2 model (continuous trace) for 4 minutes in the heating. Figure 2 (middle) shows the observed ion temperature (circles) and electron temperature (crosses) along with the three traces generated by SAM12 model.

[13] In order to improve agreement between the model and observations the neutral density in the model was adjusted so that the computed f_oF_2 peak matches the ob-

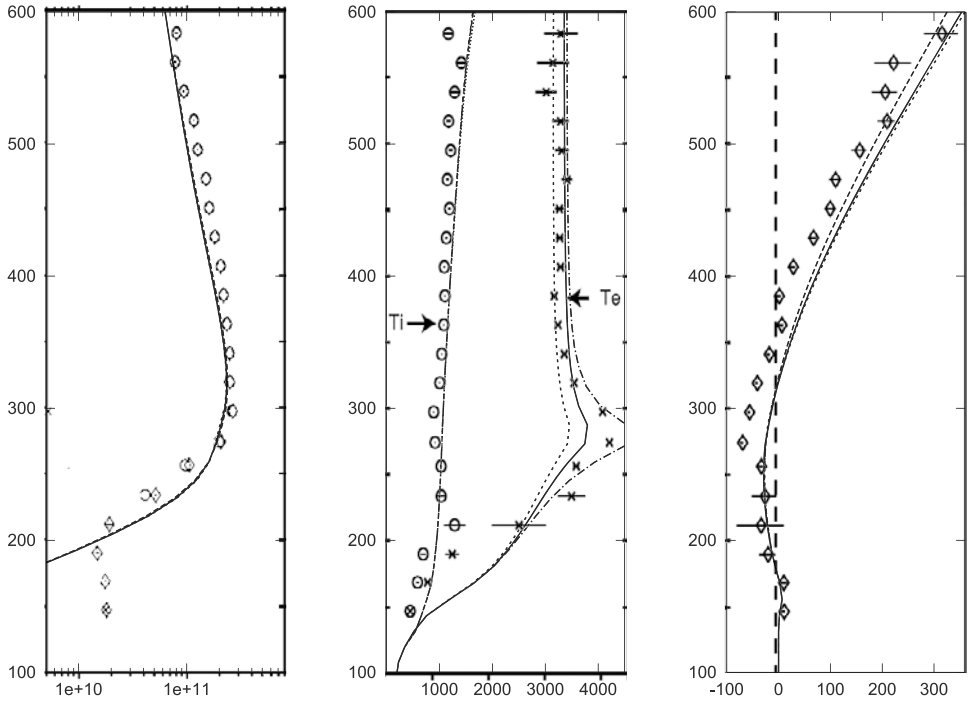

Figure 2. (left) The observed altitude profile of the electron density (circles) and the one computed by SAMI2 (continuous trace) for the four minute time interval starting on at 10/07/99 at 19:24:00 UT. (middle) The observed ion temperature (circles) and electron temperature (crosses) along with the three traces generated by the SAMI2 model. The dashed, solid, and dot-dashed line corresponds to the absorption efficiencies $\mu = 0.16$, 0.32 and 0.64 respectively. (right) The observed ion velocity (diamonds) along with the three traces which correspond to the computations made at $\mu = 016$, 0.32 and 0.64 (from left to right).

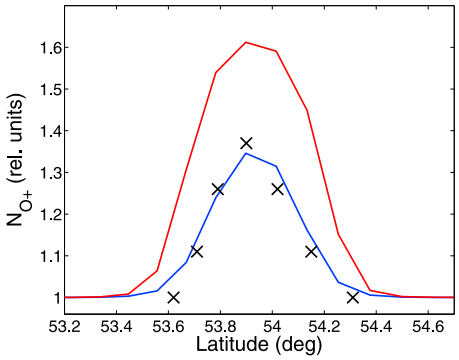

Figure 3. Relative changes in the density of O^+ ions computed for the two different absorption efficiencies μ = 0.17 and 0.29. The crosses show DEMETER observations reported by *Frolov et al.* [2008].

servations. For this purpose we have reduced the density of the atomic oxygen in the model by 50%. Such an approach is justified by the fact that SAMI2 uses averaged model values of the neutral density which may not very accurate. The adjustment leads to significant changes in the electron temperature and affects the vertical velocity only slightly. The dashed, solid, and dot-dashed lines in Figure 2 corresponds to the absorption efficiencies μ = 0.16, 0.32 and 0.64, respectively. Note that the changes in μ affect only the values of electron temperature, while the ion temperature remains unperturbed during a relatively short heating pulse. Figure 2 (right) shows the observation of the ion velocity (diamonds) along with the three traces which correspond to the computations made at different absorption efficiencies μ = 0.16, 0.32 and 0.64 (from the left to right). Also, in this case the HF heating duration did not exceed the time scale of $\mathbf{E} \times \mathbf{B}$ drift and thus the energy loss due to horizontal transport can be neglected.

[14] Figure 2 reveals that (1) HF heating with the absorption efficiencies μ = 0.3–0.6 drives perturbations of the electron temperature in good agreement with those detected by the ISR and (2) The computed ion velocity fits well with the observations. Namely, it shows that the ion velocity is negative below the heating region, and positive above it. A strong electron heating increases the electron pressure and pushes the plasma both down and upward from the heated region. Thus below this region the ion velocity is negative (downward directed), while above the region it is positive (upward directed) and its value increases with altitude since the plasma propagates in the ionosphere of decreasing density.

3.2. Comparison With SURA Experiments

[15] *Frolov et al.* [2008] reported the detection of plasma ducts by the DEMETER satellite overflying the SURA HF-heater. In fact, ducts were detected when the heater operated at 4.3 MHz, and at ERP = 80 MW, while the half-power beam width was 12° on 05/01/06. The ionosphere was quiet, Kp = 0, and the heating wave was reflected at 230 km, below the f_0F_2 peak.

[16] We conducted SAMI2 runs for this day for SURA location (56°N, 46°E) using the specified characteristics of the HF-heater. The heating began 10 minutes before the DEMETER overfly at 18:28:39 UT, and lasted for 15 minutes. Figure 3 shows the relative changes in the density of O^+ ions computed for the two different pumping rates q = 1,000 and 1,700 K/s which correspond to the absorption efficiency μ = 0.17 and 0.29 respectively. The increase in O^+ density was then checked against the DEMETER observations shown by crosses. The latter data were derived from the DEMETER observations of the time series of O^+ density [*Frolov et al.*, 2008]. We converted these data into the relative ion density by dividing them by the value of the unperturbed O^+ density measured outside the duct. In addition, we presented the relative O^+ density as a function of latitude by taking into account the orbital velocity v = 7 km/s of DEMETER. Figure 3 shows a good agreement between the observations and model for the case of the absorption efficiency μ = 0.17. Note that similar HF heating experiments were conducted at HAARP using Demeter as a diagnostic tool [*Milikh et al.*, 2008].

3.3. Concluding Remarks

[17] Recently modified SAMI2 numerical model was validated by comparison with two well documented experiments. One experiment, conducted at the SURA heating facility, used the low orbit satellite DEMETER as a diagnostic tool to measure the electron and ion temperature and density along the overflying satellite orbit close to the magnetic zenith of the HF-heater. The second experiment, conducted at the EISCAT HF facility and diagnosed by the EISCAT ISR, measured the vertical profiles of the electron and ion temperature between 150–600 km. The model reproduces the observations with high accuracy, which indicates its potential as a key tool for study of the artificial ducts, and to guide future observational campaigns. In addition, the model predicts that the ionospheric HF heating could produce strong perturbations of the plasma pressure which will then transform into magnetic field perturbations that could be detected by low orbit satellites having on-board magnetometers such as DMSP. Moreover by checking the model results against the ISR or satellite made observations one can assess efficiency of the duct production, namely what fraction of the radio beam energy was pumped into the ducts.

[18] **Acknowledgments.** The work was supported by DARPA via a subcontract N684228 with BAE Systems. It was also supported by the ONR grant NAVY.N0017302C60 and by the ONR MURI grant N000140710789. The work of A.D. was supported in part by the Russian Academy of Sciences (the Program "Plasma Processes in the Solar System").

References

Berthelier, J. J., et al. (2006a), ICE, the electric field experiment on DEMETER, *Planet. Space Sci.*, *54*, 456–471, doi:10.1016/j.pss.2005.10.016.

Berthelier, J. J., et al. (2006b), IAP, the thermal plasma analyzer on DEMETER, *Planet. Space Sci.*, *54*, 487–501, doi:10.1016/j.pss.2005.10.018.

Carpenter, D. L., M. A. Spasojević, T. F. Bell, U. S. Inan, B. W. Reinisch, I. A. Galkin, R. F. Benson, J. L. Green, S. F. Fung, and S. A. Boardsen (2002), Small-scale field-aligned plasmaspheric density structures inferred from the Radio Plasma Imager on IMAGE, *J. Geophys. Res.*, *107*(A9), 1258, doi:10.1029/2001JA009199.

Frolov, V. L., et al. (2008), Satellite measurements of plasma density perturbations induced in the topside ionosphere by high-power HF radio waves from the "SURA" heating facility, *Radiophys. Quantum Electron.*, *51*(11), 825–833.

Gurevich, A. V., A. V. Lukyanov, and K. P. Zybin (1996), Anomalous absorption of powerful radio waves on the striations developed during ionospheric modification, *Phys. Lett. A*, *211*, 363–372, doi:10.1016/0375-9601(95)00970-1.

Gustavsson, B., et al. (2001), First tomographic estimate of volume distribution of HF-pump enhanced airglow emission, *J. Geophys. Res.*, *106*(A12), 29,105–29,123, doi:10.1029/2000JA900167.

Huba, J. D., G. Joyce, and J. A. Fedder (2000), Sami2 is another model of the ionosphere (SAMI2): A new low-latitude ionosphere model, *J. Geophys. Res.*, *105*(A10), 23,035–23,053, doi:10.1029/2000JA000035.

Koons, H. C. (1989), Observations of large-amplitude, whistler-mode wave ducts in the outer plasmasphere, *J. Geophys. Res.*, *94*(A11), 15,393–15,397, doi:10.1029/JA094iA11p15393.

Milikh, G. M., K. Papadopoulos, H. Shroff, C. L. Chang, T. Wallace, E. V. Mishin, M. Parrot, and J. J. Berthelier (2008), Formation of artificial ionospheric ducts, *Geophys. Res. Lett.*, *35*, L17104, doi:10.1029/2008GL034630.

Perrine, R. P., G. M. Milikh, K. Papadopoulos, J. D. Huba, G. Joyce, M. Swisdak, and Y. Dimant (2006), An interhemispheric model of artificial ionospheric ducts, *Radio Sci.*, *41*, RS4002, doi:10.1029/2005RS003371.

Rietveld, M. T., M. J. Kosch, N. F. Blagoveshchenskaya, V. A. Kornienko, T. B. Leyser, and T. K. Yeoman (2003), Ionospheric electron heating, optical emissions, and striations induced by powerful HF radio waves at high latitudes: Aspect angle dependence, *J. Geophys. Res.*, *108*(A4), 1141, doi:10.1029/2002JA009543.

Streltsov, A. V., M. Lampe, W. Manheimer, G. Ganguli, and G. Joyce (2006), Whistler propagation in inhomogeneous plasma, *J. Geophys. Res.*, *111*, A03216, doi:10.1029/2005JA011357.

A. G. Demekhov, Institute of Applied Physics, Russian Academy of Sciences, 46 Ulyanov St., Nizhny Novgorod, 603950, Russia.

J. D. Huba, Naval Research Laboratory, Washington, DC 20375-5320, USA.

G. Joyce, Icarus Research, Inc., P.O. Box 30780, Bethesda, MD 20824-0780, USA.

K. Papadopoulos, G. M. Milikh, and A. Vartanyan, Department of Astronomy, University of Maryland, College Park, MD 20742, USA. (milikh@astro.umd.edu)